Photoluminescence Imaging Characterization of Thin-Film InP

Steve Johnston[1], Alyssa Allende Motz[1,2], James Moore[3], Maxwell Zheng[4], Ali Javey[4], and Peter Bermel[3]

[1]National Renewable Energy Laboratory, Golden, CO, 80401, U.S.A.
[2]Colorado School of Mines, Golden, CO, 80401, U.S.A.
[3]Purdue University, West Lafayette, IN, 47907, U.S.A.
[4]University of California, Berkeley, CA, 94720, U.S.A.

***Abstract* — Indium phosphide grown using a novel vapor-liquid-solid method is a promising low-cost material for III-V single-junction photovoltaics. In this work, we characterize the properties of these materials using photoluminescence (PL) imaging, time-resolved photoluminescence (TRPL), and microwave-reflection photoconductive decay (μ-PCD). PL image data clearly shows the emergence of a self-similar dendritic growth network from nucleation sites, while zoomed-in images show grain structure and grain boundaries. Single photon TRPL data shows initial surface-dominated recombination, while two-photon excitation TRPL shows a lifetime of 10 ns. Bulk carrier lifetime may be as long as 35 ns as measured by μ-PCD, which can be less sensitive to surface recombination.**

***Index Terms* — charge carrier lifetime, grain boundaries, imaging, indium phosphide, photoconductivity, photoluminescence, photovoltaic cells.**

I. Introduction

InP has a direct band gap (1.34 eV, ~920 nm) with strong light absorption and a high open-circuit voltage that makes it an efficient photovoltaic material, with potential for further improvement [1]. Historically, making InP wafers or epitaxial growth of monocrystalline InP thin films has been a highly expensive process, which has had limited testing and adoption. However, the more recently developed technique of vapor-liquid-solid (VLS) growth on metal foils is a promising low-cost alternative [2]-[3]. InP thin films of 1-3 μm thickness have recently been grown by the VLS method on Mo foils, possessing grain sizes up to 100 μm. Here, we characterize these InP thin films using three techniques: photoluminescence (PL) imaging [4]-[5], time-resolved photoluminescence (TRPL) [6]-[7], and microwave-reflection photoconductive decay (μ-PCD) [7]. PL imaging provides spatial resolution of non-uniformities, crystal structures, grain boundaries, and localized defects. Intensities often correlate to carrier lifetime and solar cell performance [8]-[9]. TRPL and μ-PCD each measure transient recombination of excess carriers and give a carrier lifetime, which is indicative of material quality. TRPL monitors excess carriers through radiative recombination, while μ-PCD is sensitive to the increased conductivity due to excess carriers. The techniques are often complementary, and one can be used to verify the other. However, differences can also be used to further understand recombination processes, such as surface and bulk recombination, as will be discussed later.

II. Experiment

The sample is a VLS-grown InP film with a starting In thickness of 3 μm and a 30 nm SiO_2 cap layer. Figure 1 shows the thin-film InP sample, where the field of view is 1 cm in width. The image of Fig. 1(a) is a room-light image of the sample, while a PL image is shown in Fig. 1(b). These images are collected using a Princeton Instruments PIXIS 1024BR Si-charge-coupled-device camera. The camera is cooled to -60°C, which reduces background counts, and the total background and read-out noise is only about 1% of the 16-bit pixel capacity. The PL image is collected while the sample is housed in a dark enclosure. With minimal background counts, no background image is needed for

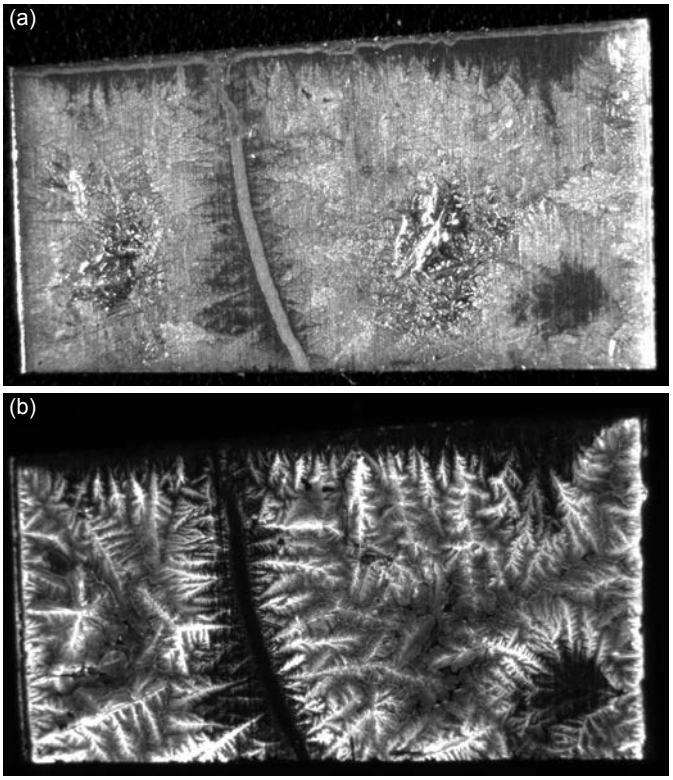

Fig. 1. The upper image (a) shows a room-light image of the thin-film InP sample. The lower image (b) shows the PL image. The sample is 1 cm wide.

978-1-4799-7944-8/15/$31.00 ©2015 IEEE

subtraction, so the images are collected using a single exposure time.

Excitation light is provided by fiber-coupled 810-nm laser diodes or 532-nm laser diodes such that continuous light is uniformly illuminated upon the sample. A long-pass filter is used to block reflections of excitation light while allowing the PL emission to enter the camera. Image acquisition times can range from seconds to minutes, and for this sample in particular, exposure times of just a couple seconds were adequate to collect the PL images and nearly fill the detector pixels. Uncropped images have a resolution of 1024 x 1024 pixels.

In Fig. 1(b), bright regions correlate to stronger PL emission, as the PL intensity is proportional to excess carrier lifetime and doping. There may also be variation in material thickness and optical properties. The PL image shows evidence of self-similar dendritic growth from nucleation sites, as has been observed during growth by optical microscopy [2].

For high spatial resolution, we have used a Mitutoyo 20X microscope objective with 0.40 numerical aperture and 20 mm working distance coupled with a Navitar Zoom 6000 lens. This lens system has the capability to zoom in with a field of view from ~1.3 mm down to ~190 μm. A photograph of the PL imaging experimental setup with the PIXIS camera and Navitar/Mitutoyo lens system is shown in Fig. 2. There are four laser diode units that illuminate the sample from opposite sides. The light from each laser diode strikes the sample at a shallow angle to prevent shadowing from the microscope objective. An advantage of this configuration is that any strong specular reflections are angled away from the lens; however, surface features such as roughness, scratches, or dust, can cause a strong reflection of light into the camera lens. In this case, the filter is often not sufficient to completely block the reflected light. It is also a disadvantage when the light strikes the sample at a shallow angle, and the excitation intensity is not uniform. Multiple light sources from opposite angles are used to help compensate and create a more uniform excitation.

Figure 3 shows the PL image of the left side of the InP sample. An example of a PL image using the microscope objective zoom lens is shown in the inset of Fig. 3. This image is 1.3 mm across, which is the largest field of view for this lens.

By further zooming in, more detailed spatial resolution shows features within grains and grain boundaries. Using a field of view of ~450 x 450 μm, PL images of two different regions from the inset area of Fig. 3 are shown in Fig. 4. The PL image of Fig. 4(a) is from the upper part of the inset of Fig. 3. Fig. 4(b) is from the middle and lower part of the Fig. 3 inset. These zoom images show grain boundaries, dark and bright grains, and linear stripe features within the grains that may parallel growth or crystal twinning.

Fig. 2. Photograph of the PL imaging experimental setup showing the PIXIS camera with Navitar and Mitutoyo lens system for close up zoom and high spatial resolution.

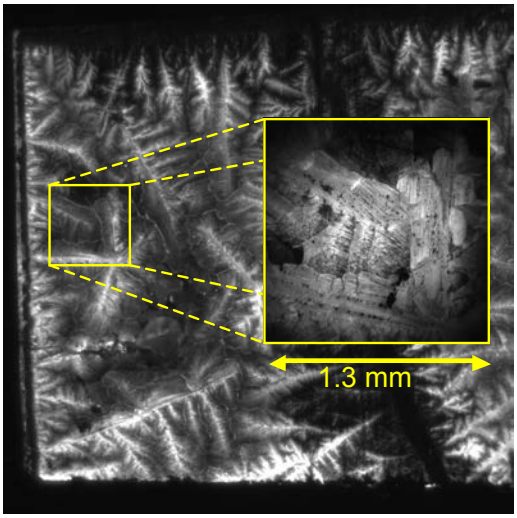

Fig. 3. PL image of the left side of the thin-film InP sample. The field of view is approximately 8 mm. The inset box shows higher spatial resolution when zooming in using the Navitar/Mitutoyo lens system. The field of view is 1.3 mm.

978-1-4799-7944-8/15/$31.00 ©2015 IEEE

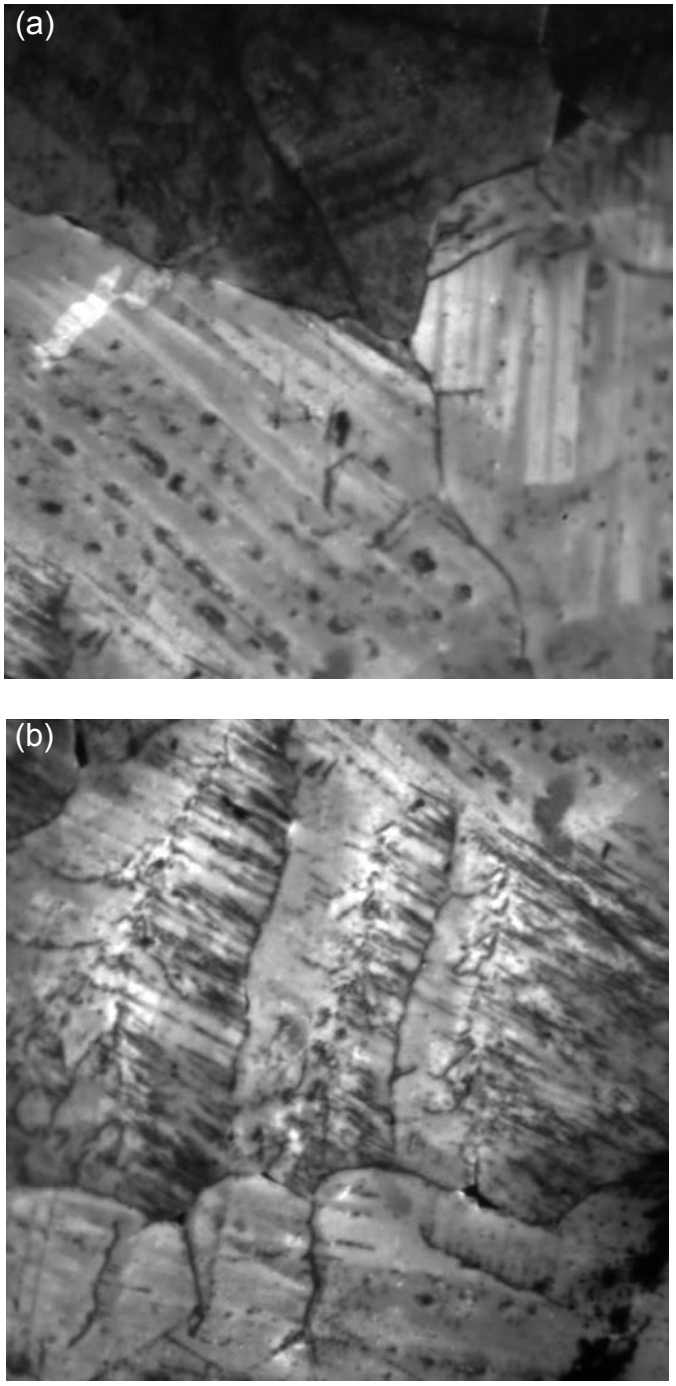

Fig. 4. High resolution PL images with a field of view of ~450 μm x 450 μm. The regions are from the top half (a) and bottom half (b) of the inset PL image in Fig. 3.

PL intensities from a PL image often show correlation to minority-carrier lifetime, diffusion length, and cell voltage [8]-[9]. Additionally, more quantitative results can be achieved using other measurements to supplement the images. We have measured TRPL on the thin-film InP sample using a commercial femtosecond pulsed laser system with tunable optical parametric amplifier (OPA). The laser is a Light Conversion Ltd. PHAROS with fundamental wavelength of 1030 nm, pulse width of 300 fs, and repetition rate of 1.1×10^6 pulses per second. The ORPHEUS OPA is used to tune to particular wavelengths ranging from ultraviolet to infrared. Optical filters allow longer wavelength light to be collected to an avalanche photodiode detector. When using two-photon excitation, filters are used to block the longer excitation wavelengths and allow collection of the shorter-wavelength sample photoluminescence. We have used a 920-nm bandpass filter and additional long-pass or short-pass filters as needed. A PicoQuant 'PicoHarp 300' time-correlated single-photon counting module is used to construct the decay curve, and the overall system response is ~0.1 ns. The measurement spot size is roughly 0.2 mm.

Figure 5 shows the PL decay curves for one-photon absorption using an excitation wavelength of 640 nm and two-photon absorption using 1500 nm. For single photon absorption of red, 640-nm light, the absorption coefficient is ~5×10^4 cm^{-1} [10]-[11]. This results in 90% of the carriers being excited in the top ~0.5 μm of the sample, and recombination is then strongly dependent upon the top surface/interface passivation. The initial decay represents excess carriers that recombine at the top interface, and here, the decay time is 1.7 ns. Using $\tau_S = d/S$, where τ_S is 1.7 ns, d is the thickness of 0.5 μm, and S is the surface recombination velocity, then $S = 3 \times 10^4$ cm/s. This estimate compares reasonably well to previous reports of low surface recombination velocity for InP [12]-[16].

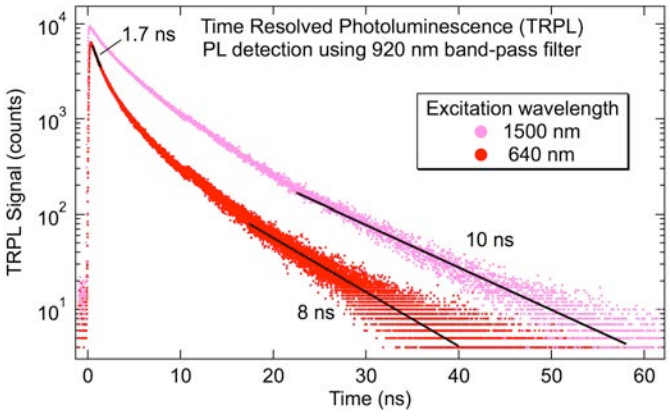

Fig. 5. TRPL data for both one-photon excitation (640 nm) and two-photon excitation (1500 nm) for the thin-film InP sample.

We now consider the PL decay at longer times. After the initial decay, excess carriers rapidly deplete near the surface, so the decay becomes more dominated by the film's bulk recombination. At longer times, the decay rate for the single-photon absorption is around 8 ns. Two-photon excitation is a weak absorption process where longer wavelength light excites excess carriers. [17] Weak absorption leads to more

978-1-4799-7944-8/15/$31.00 ©2015 IEEE

uniform carrier excitation throughout the thickness of the film. While carriers near the surfaces can quickly recombine through surface states, more carriers are distributed deeper in the bulk of the film, and the resulting decay can be better dominated by bulk recombination. Figure 5 shows a two-photon TRPL decay curve where the excitation wavelength is 1500 nm. The initial decay is not as fast due to the more uniform distribution of carriers, and at longer times, the decay rate is around 10 ns, which compares fairly well to the low injection decay time of the single-photon TRPL measurement. The values of S and lifetime are in close agreement with results of modeling and PL excitation measurements performed on similar thin-film InP samples [18].

It has previously been shown that even if carriers are uniformly distributed throughout the thickness of the sample, detecting PL can have a limited depth of measurement due to self-absorption [7]. Photons generated by carrier recombination deep within the bulk can be reabsorbed before reaching the surface. When the depth is limited by self-absorption, the measurement can be more influenced by surface/interface recombination. Thus, a supplemental or alternative method for monitoring carrier recombination is appropriate to consider, such as photoconductivity.

For the μ-PCD technique, the sample's photoconductivity due to excess carriers is characterized by monitoring microwave power that is reflected from the sample, in this case, through the front side of the sample co-linear with the laser light excitation. A signal generator produces a 20-GHz signal that propagates through a microwave directional coupler and waveguide and is directed onto the sample. An E/H-plane tuner consisting of sliding shorts is used to minimize dark conductivity reflected power. Photoconductivity-induced reflected power during each laser pulse is detected after the coupler/reflectometer and rectified using a diode detector, such as a Krytar 302A zero-bias Schottky detector. The detector's 3-pF output capacitance terminated into 50 Ω gives a rise time of ~1 ns. This signal is amplified and output to an oscilloscope. The 1-ns system response is as fast as the laser pulse, which in this case, is a Nd:YAG Q-switched laser used to pump an optical parametric oscillator (OPO) with a resulting laser pulse width of 3-5 ns.

The thin-film InP sample is measured by μ-PCD, and the photoconductivity decay curves are shown in Fig. 6. The measurement spot is about 5 mm x 1 cm, which is roughly the size of the sample. A wide range of laser wavelengths are used for carrier excitation to sweep from strong absorption near the top surface to very weak absorption and more uniform excess carrier distribution throughout the film thickness. For short wavelengths, such as 770 nm to 920 nm, the absorption coefficient is greater than 10^4 cm^{-1}, and carriers are excited near the top surface. The μ-PCD lifetime is about 15 ns, which is slightly longer than that measured by TRPL, but comparable. Due to the longer laser pulse and longer system response, the μ-PCD technique cannot resolve any initial fast decay of a few nanoseconds or less. But, the μ-PCD technique can sense photoconductivity throughout the film thickness, so it can be more sensitive than TRPL to carriers deep in the film. As the laser excitation is further tuned to longer wavelengths, absorption quickly decreases, and carrier concentration decreases but also becomes more uniformly distributed throughout the sample thickness. The laser power is ~3.5 +/- 0.5 mJ/pulse for all of the wavelengths, and the spot size is roughly 2 cm in diameter. As the excitation wavelength increases, the excess carrier decay times increase until the absorption becomes too weak to generate a significant signal. The uniform carrier generation and ability of μ-PCD to detect deep within the film suggest the bulk lifetime to be as high as 35 ns.

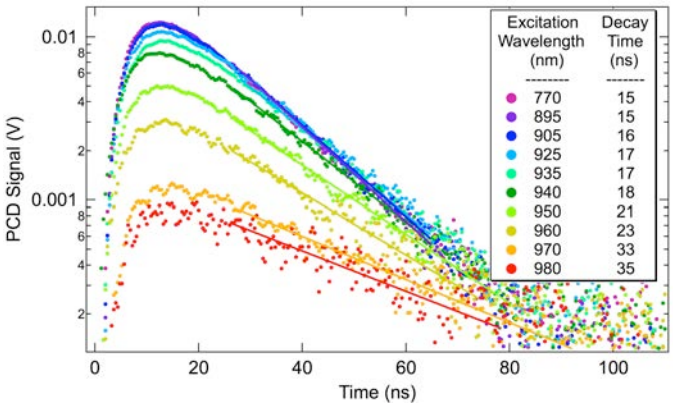

Fig. 6. Wavelength-dependent excitation of carriers used for μ-PCD.

For the μ-PCD measurement, the increasing wavelength promoted a more uniform excess carrier distribution, but it also reduced the total generation of excess carriers. The changing decay rates could be either a function of carrier distribution or injection level. So, for comparison, μ-PCD decay rates as a function of only the injection level are shown in Fig. 7.

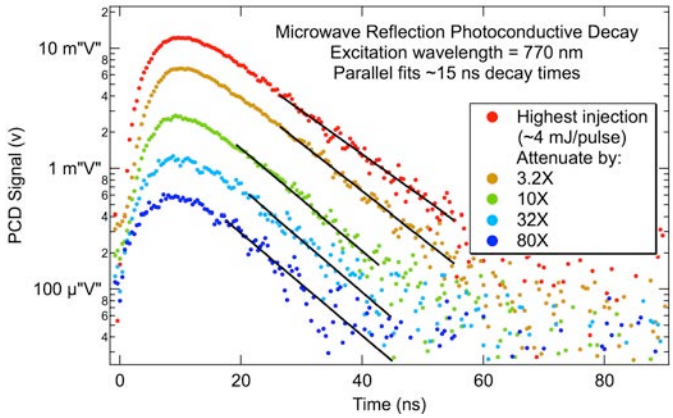

Fig. 7. Injection-level variation of μ-PCD using 770 nm excitation wavelength.

978-1-4799-7944-8/15/$31.00 ©2015 IEEE

In Fig. 7, the same starting conditions (wavelength of 770 nm and power level near 4 mJ/pulse) give a decay rate of ~15 ns, as shown in Fig. 6. Using the same wavelength, the power is reduced by placing neutral density filters into the laser beam. The signal decreases as the injection level is reduced by up to a factor of 80. This amount of μ-PCD signal reduction is comparable to the amount of signal reduction in Fig. 6, so it is assumed that the overall injection level has been reduced by a similar amount. As the injection level is reduced, the decay curves remain parallel, and the decay times are consistently near the starting 15 ns value. This gives further evidence that the decay times of Fig. 6 are increasing as the excess carriers are more uniformly distributed through the sample thickness, and that the effective lifetime is less weighted by excess carrier recombination at the top surface and more dominated by the sample's bulk lifetime. Further measurements may still be required before definitively stating a bulk lifetime of 35 ns, since carrier trapping and emission from shallow defect levels can prolong photoconductivity and lead to longer decay times than the actual carrier recombination rates. Any potential trapping artifact of the μ-PCD signal might be disclosed if measurements as a function of sample temperature were performed.

III. Summary

A thin-film InP sample has been characterized using PL imaging and minority-carrier lifetime measurement techniques. The PL images showed dendritic growth on the large cm-scale, while zoomed-in images showed grain structure and grain boundaries with μm resolution. PL imaging often shows correlation to minority-carrier lifetime and material quality; thus, it is a useful technique for rapid evaluation of growth and processing. TRPL has been used to characterize surface recombination and effective bulk lifetimes of the InP film. A surface recombination velocity of $3x10^4$ cm/s and a lifetime near 10 ns are similar results to previously reported values. Photoconductivity decay measurements showed similar values (~15 ns) to TRPL when short excitation wavelengths were used to create excess carriers. However, long excitation wavelengths with weak absorption generated excess carriers throughout the InP film, and the bulk-dominated carrier lifetime has been measured by μ-PCD to possibly be as high as 35 ns, although further work is needed to verify this value.

Acknowledgements

The InP thin film growth was funded by the Bay Area Photovoltaics Consortium (BAPVC) through DOE cooperative agreement No. DE EE 0004946. This work was supported by the National Renewable Energy Laboratory as a part of the Non-Proprietary Partnering Program under Contract No. DE-AC36-08-GO28308 with the U.S. Department of Energy. The U.S. Government retains and the publisher, by accepting the article for publication, acknowledges that the U.S. Government retains a nonexclusive, paid up, irrevocable, worldwide license to publish or reproduce the published form of this work, or allow others to do so, for U.S. Government purposes.

References

[1] X. Yin, C. Battaglia, Y. Lin, K. Chen, M. Hettick, M. Zheng, C.-Y. Chen, D. Kiriya, and A. Javey, "19.2% Efficient InP Heterojunction Solar Cell with Electron-Selective TiO_2 Contact," *ACS Photonics*, vol. 1, pp. 1245-1250, 2014.

[2] R. Kapadia, Z. Yu, H.-H. H. Wang, M. Zheng, C. Battaglia, M. Hettick, D. Kiriya, K. Takei, P. Lobaccaro, J. W. Beeman, J. W. Ager, R. Maboudian, D. C. Chrzan, and A. Javey, "A direct thin-film path towards low-cost large-area III-V photovoltaics," *Scientific Reports*, vol. 3:2275, pp. 1-7, 2013.

[3] D. Kiriya, M. Zheng, R. Kapadia, J. Zhang, M. Hettick, Z. Yu, K. Takei, H.-H. H. Wang, P. Lobaccaro, and A. Javey, "Morphological and spatial control of InP growth using closed-space sublimation," *J. Appl. Phys.*, vol. 112, pp. 123102-1-123102-6, 2012.

[4] T. Trupke, R. A. Bardos, M. C. Schubert, and W. Warta, "Photoluminescence imaging of silicon wafers." *Appl. Phys. Lett.*, vol. 89, pp. 044107-1-044107-3, 2006.

[5] S. W. Johnston, N. J. Call, B. Phan, and R. K. Ahrenkiel, "Applications of imaging techniques for solar cell characterization," in *34th IEEE Photovoltaic Specialists Conference,* 2009, pp. 276-281.

[6] W. K. Metzger, D. Albin, D. Levi, P. Sheldon, X. Li, B. M. Keyes, and R. K. Ahrenkiel, "Time-resolved photoluminescence studies of CdTe solar cells," *J. Appl. Phys.*, vol. 94, pp. 3549-3555, 2003.

[7] S. Johnston, K. Zaunbrecher, R. Ahrenkiel, D. Kuciauskas, D. Albin, and W. Metzger, "Simultaneous Measurement of Minority-Carrier Lifetime in Single-Crystal CdTe Using Three Transient Decay Techniques," *IEEE J. Photovoltaics*, vol. 4, pp. 1295-1300, 2014.

[8] S. Johnston, T. Unold, I. Repins, A. Kanevce, K. Zaunbrecher, F. Yan, J. V. Li, P. Dippo, R. Sundaramoorthy, K. M. Jones, and B. To, "Correlations of $Cu(In,Ga)Se_2$ imaging with device performance, defects, and microstructural properties," *J. Vac. Sci. Technol. A*, vol. 30, pp. 04D111-1-04D111-6, 2012.

[9] S. Johnston, H. Guthrey, F. Yan, K. Zaunbrecher, M. Al-Jassim, P. Rakotoniaina, and M. Kaes, "Correlating Multicrystalline Silicon Defect Types Using Photoluminescence, Defect-band Emission, and Lock-in Thermography Imaging Techniques," *IEEE J. Photovoltaics*, vol. 4, pp. 348-354, 2014.

[10] W. J. Turner, W. E. Reese, and G. D. Pettit, *Phys. Rev.*, vol. 136, pp. A1467-1470, 1964.

[11] Edward D. Palik, *Handbook of Optical Constants of Solids*. New York, New York: Academic Press, 1985.

[12] H. C. Casey and E. Buehler, "Evidence for low surface recombination velocity on n-type InP," *Appl. Phys. Lett.*, vol. 30, p. 247, 1977.

[13] S. Bothra, S. Tyagi, S. K. Ghandhi, and J. Borrego, "Surface recombination velocity and lifetime in InP measured by transient microwave reflectance," in *21st IEEE Photovoltaic Specialists Conference*, 1990, pp. 404 – 408.

[14] S. Bothra, S. Tyagi, S. K. Ghandhi, and J. M. Borrego, "Surface recombination velocity and lifetime in InP," *Solid-State Electron.*, vol. 34, pp. 47–50, 1991.

[15] Y. Rosenwaks, Y. Shapira, and D. Huppert, "Evidence for low intrinsic surface-recombination velocity on p-type InP," *Phys. Rev. B*, vol. 44, pp. 13097–13100, 1991.
[16] Y. Rosenwaks, Y. Shapira, and D. Huppert, "Picosecond time-resolved luminescence studies of surface and bulk recombination processes in InP," *Phys. Rev. B*, vol. 45, pp. 9108–9119, 1992.
[17] R. L. Sutherland, *Handbook of Nonlinear Optics, 2nd ed*. New York, New York: Marcel Dekker, 2003.
[18] X. Wang, J. Bhosale, J. Moore, R. Kapadia, P. Bermel, A. Javey, and M. Lundstrom, "Photovoltaic Material Characterization With Steady State and Transient Photoluminescence," IEEE J. of Photovoltaics, vol. 5, pp. 282-287, 2015.

978-1-4799-7944-8/15/$31.00 ©2015 IEEE